



Bose-Einstein condensation of photons in microcavity plasmasJ. L. Figueiredo ^{*}, J. T. Mendonça, and H. Terças *GoLP - Instituto de Plasmas e Fusão Nuclear, Instituto Superior Técnico, Universidade de Lisboa, 1049-001 Lisboa, Portugal*

(Received 28 April 2023; accepted 21 June 2023; published 17 July 2023)

Bose-Einstein condensation of a finite number of photons propagating inside a plasma-filled microcavity is investigated. The nonzero chemical potential is provided by the electrons, which induces a finite photon mass and allows condensation to occur. We derive an equation that models the evolution of the photon-mode occupancies, with Compton scattering taken into account as the mechanism of thermalization. The kinetic evolution of the photon spectrum is solved numerically, and we find evidence of condensation down to nanosecond timescales for typical microplasma conditions, $n_e \sim 10^{14}$ – 10^{15} cm⁻³. The critical temperature scales almost linearly with the number of photons, and we find high condensate fractions at microcavity-plasma temperatures, for experimentally achievable cavity lengths (100–500 μm) and photon numbers (10^{10} – 10^{12}).

DOI: [10.1103/PhysRevE.108.L013201](https://doi.org/10.1103/PhysRevE.108.L013201)

Introduction. Over the past years, Bose-Einstein condensation has been accomplished with atomic species, including ⁷Li [1], spin-polarized ¹H [2], metastable ⁴He [3], and ⁴¹K [4]. Despite the remarkable advances on the experimental realization of Bose-Einstein condensates (BECs), the possibility of producing a condensate of photons remained elusive for a long time. The reason relies on the vanishing chemical potential of free photons, which leads to nonconservation of the number of particles during thermalization, thus preventing the second-order phase transition to occur. This problem was first circumvented in Ref. [5], where it was shown that the presence of a cavity grants the photons with an effective mass. Nevertheless, no thermalization mechanism was proposed therein. The latter was then addressed in Refs. [6,7], where experimental evidence for the formation of a photon BEC in dye-filled cavities was first reported. Later on, other authors have observed photon condensation in similar physical setups [8,9]. Such remarkable findings have motivated a number of theoretical studies, unveiling the mechanisms behind photon condensation with dye molecules [10–14] and atomic media [15,16].

An alternative physical medium in which one could imagine photons to undergo condensation is the plasma, where a finite mass is also established [17–20]. Contrary to experiments with optical cavities, photon condensation in plasmas was thought to be a *bulk* phenomenon, arising in homogeneous and unbounded systems [21]. This is particularly relevant in the astrophysical context, where external trapping potentials are absent. Indeed, this possibility was first considered by Zel’dovich and Levich in 1968 [22], in relation to the distortion of the cosmic microwave background radiation through inverse Compton scattering—the so-called Sunyaev-Zel’dovich effect [23]. However, the question of photon condensation in finite-sized plasma systems has yet to be proposed.

In this Letter, we investigate photon thermalization in a microcavity plasma, and find evidence of high-temperature condensation. The system under study takes advantage of both the photon mass, $m_{\text{ph}} = \hbar\omega_p/c^2$ with ω_p the plasma frequency, and the boundary conditions induced by the cavity, which lead to a discretization of photon modes. The mode discreteness yields a finite critical temperature despite the system being effectively one dimensional. We derive and solve the kinetic equations accounting for the evolution of the photon spectrum, with Compton scattering acting as the thermalization mechanism. After integrating out the electron degrees of freedom, we obtain a set of coupled equations for the photon modes dressed by the plasma. For sufficiently high photon intensities, we find macroscopic fractions of particles occupying the ground state. The evolution equation of photon modes becomes nonlinear due to photon degeneracy, which results in condensation times that decrease rapidly (down to tens of nanoseconds) with increasing photon intensities. We find sufficiently small condensation times to render plasma absorption processes, as well as cavity losses, negligible, allowing for the condensate to form. Remarkably, the critical temperatures are extremely high, when compared to the ones of customary BEC experiments with identical photon numbers [7]. We find that those temperatures are also compatible with those of microdischarge plasmas, which opens the possibility of conceiving condensation directly inside a microcavity plasma [24]. Since the microcavity can be easily built into a microelectronic circuit, the proposed mechanism finds a plethora of applications in a future generation of photon-based circuits and radiation sources.

Plasma wave equations. We start by revising the theory of electron-photon coupling in a plasma. Essentially, the effect of the plasma is to modify the refraction index of the medium, which becomes $n(\omega) = (1 - \omega_p^2/\omega^2)^{1/2}$, with $\omega_p^2 = e^2 n_e / (\epsilon_0 m_e)$ and e being the elementary charge, n_e the electron density, ϵ_0 the vacuum permittivity, and m_e the electron mass. The frequency becomes space and time dependent, through the local electron density $n_e \equiv n_e(\mathbf{r}, t)$. Conversely, the ion

^{*}jose.luis.figueiredo@tecnico.ulisboa.pt

motion is negligible due their high inertia, and the photon dynamics is mostly determined by the electrons. The photon dispersion relation follows from $\omega = ck/n(\omega)$ [25].

To derive the latter, we resort to Maxwell equations. We start from Ampère's law

$$\nabla \times \mathcal{B} = \frac{1}{c^2} \partial_t \mathcal{E} + \mu_0 \mathbf{J}, \quad (1)$$

with \mathcal{B} denoting the magnetic field, \mathcal{E} the electric field, and \mathbf{J} the charge current density. The current is responsible for the coupling of photons with the plasma via $\mathbf{J} = \sum_j Q_j n_j \mathbf{u}_j$, with j running over the different species (electron e and ion i) of charge Q_j , density n_j , and velocity \mathbf{u}_j . The fields n_j and \mathbf{u}_j evolve with their own classical equations of motion coupled to the electromagnetic fields,

$$\partial_t n_j + \nabla \cdot (n_j \mathbf{u}_j) = 0 \quad (2)$$

and

$$\partial_t \mathbf{u}_j + \mathbf{u}_j \cdot \nabla \mathbf{u}_j = \frac{Q_j}{m_j} (\mathcal{E} + \mathbf{u}_j \times \mathcal{B}) - \frac{1}{m_j n_j} \nabla P_j, \quad (3)$$

where P_j is the pressor tensor. Following the usual prescription, we write the electromagnetic fields in terms of the potentials ϕ and \mathbf{A} , $\mathcal{E} = -\nabla\phi - \partial_t \mathbf{A}$ and $\mathcal{B} = \nabla \times \mathbf{A}$. Replacing for those in Eq. (1) and neglecting the slow ion motion leads to

$$\left(\nabla^2 - \frac{1}{c^2} \partial_t^2 \right) \mathbf{A} = \frac{\omega_p^2}{c^2} \mathbf{A}. \quad (4)$$

Equation (4) takes the form of a Klein-Gordon equation, suggesting that the dressed photons are massive, in a process that is reminiscent of the Higgs-Anderson mechanism [17–20]. By Fourier transforming Eq. (4), we obtain the photon dispersion

$$\omega \equiv \omega_{\mathbf{k}} = (\omega_p^2 + c^2 k^2)^{1/2}, \quad (5)$$

which leads to the photon mass $m_{\text{ph}} = \hbar \omega_p / c^2$, scaling with the electron density as $m_{\text{ph}} \sim \sqrt{n_e}$. Equation (5) can now be compared to $\omega = ck/n$, from which we can extract the refraction index $n(\omega) = (1 - \omega_p^2/\omega^2)^{1/2}$.

Kinetic model. In the case of a fully ionized plasma, elastic electron-photon scattering is the main source of thermalization. Scattering between the photons and ions might also occur, but with a probability that is several orders of magnitude smaller and that we shall neglect here [26]. We follow the Boltzmann approach and calculate the variation of the number of particles measured by a joint distribution function $\rho(\mathbf{p}, \mathbf{k}, t)$ with electrons in mode \mathbf{p} and photons in mode \mathbf{k} , at time t . We have

$$\partial_t \rho(\mathbf{p}, \mathbf{k}, t) = J_+(\mathbf{p}, \mathbf{k}, t) - J_-(\mathbf{p}, \mathbf{k}, t), \quad (6)$$

with $J_{+(-)}$ being the number of particles per unit volume per unit time that enters (leaves) the phase-space element $d^3\mathbf{p} d^3\mathbf{k}$ centered in (\mathbf{p}, \mathbf{k}) due to a scattering event. The currents can be written as

$$J_+(\mathbf{p}, \mathbf{k}, t) = \int d^3\mathbf{p}' d^3\mathbf{k}' \rho(\mathbf{p}', \mathbf{k}', t) W(p', k' \rightarrow p, k) \times [1 + N(\mathbf{k}, t)][1 - F(\mathbf{p}, t)], \quad (7)$$

$$J_-(\mathbf{p}, \mathbf{k}, t) = \int d^3\mathbf{p}' d^3\mathbf{k}' \rho(\mathbf{p}, \mathbf{k}, t) W(p, k \rightarrow p', k') \times [1 + N(\mathbf{k}', t)][1 - F(\mathbf{p}', t)], \quad (8)$$

with $N(\mathbf{k}, t) = n_e^{-1} \int d^3\mathbf{p} \rho(\mathbf{p}, \mathbf{k}, t)$ and $F(\mathbf{p}, t) = n_{\text{ph}}^{-1} \int d^3\mathbf{k} \rho(\mathbf{p}, \mathbf{k}, t)$ denoting the photon and electron distributions with densities n_{ph} and n_e , and total number of particles N_{ph} and N_e , respectively. In writing Eq. (6), all processes leading to the nonconservation of electron number (such as impact ionization and radiative recombination or excitation) are neglected due to their small rates when compared to the scattering rates for the process of interest [27], assuming that the plasma has been produced with a large ionization degree. The factor $W(p, k \rightarrow p', k')$ is the transition rate from incoming (p, k) to final (p', k') states, with p, k, p' , and k' denoting the four-vector momenta associated with the electron and photon degrees of freedom. Additionally, the factors $1 + N$ and $1 - F$ in Eqs. (7) and (8) account for quantum degeneracy of each population, i.e., they ensure that fermions do not occupy the same state and bosons tend to occupy the same state. For the conditions considered here, electrons are nondegenerate and we may safely set $1 - F \simeq 1$. On the contrary, the photon degeneracy may not be discarded, for it results in a nonlinear term of order N^2 that is crucial to the condensation process.

Since we are interested in the dynamics of photons, it is convenient to integrate out the electron degrees of freedom. This procedure is valid as long as the correlations between electrons and photons can be neglected; in other words, when the following expansion holds,

$$\rho(\mathbf{p}, \mathbf{k}, t) \simeq F(\mathbf{p}, t)N(\mathbf{k}, t) + \text{correlations}, \quad (9)$$

with the second term on the right-hand side being much smaller than the first. Correlations are small whenever there is a separation of timescales, which in the present case amounts to having the electron gas equilibrated much faster than the photons. Under those assumptions, and invoking dynamical reversibility in the form $W(p, k \rightarrow p', k') = W(p', k' \rightarrow p, k)$, the Boltzmann equation reduces to an equation for the photon distribution function,

$$\partial_t N(\mathbf{k}) = \frac{1}{n_e} \int d^3\mathbf{p} d^3\mathbf{p}' d^3\mathbf{k}' W(p, k \rightarrow p', k') \times \{F(\mathbf{p}')N(\mathbf{k}')[1 + N(\mathbf{k})] - F(\mathbf{p})N(\mathbf{k})[1 + N(\mathbf{k}')]\}. \quad (10)$$

The amplitude for the Compton event is given by [28]

$$W = \frac{3\sigma_T n_e}{16\pi} \delta(p + k - p - k')(1 + \cos^2 \theta), \quad (11)$$

with $\sigma_T \simeq 6.65 \times 10^{-29} \text{ m}^2$ being the Thompson cross section and θ the photon scattering angle.

We proceed to apply the above equations to the case of a plasma contained inside a planar Fabry-Pérot microcavity, as depicted in Fig. 1. We introduce the discretized photon momenta $\mathbf{k} \equiv \mathbf{k}_\ell = \pi \ell \mathbf{e}_z / d$, where ℓ is an integer, \mathbf{e}_z is directed along the longitudinal axis of the cavity, and d is the distance in the \mathbf{e}_z direction. The photon frequencies are denoted by

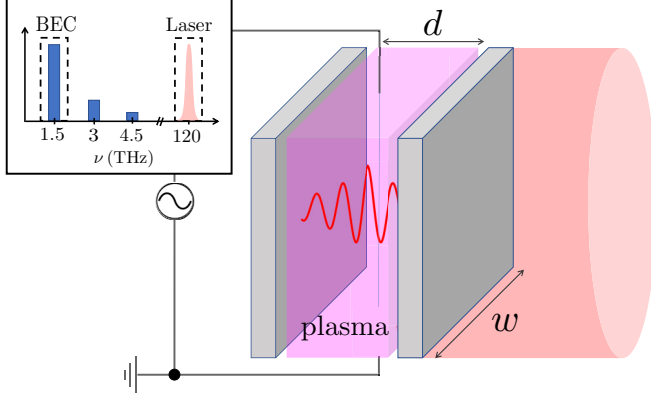


FIG. 1. Scheme of the experimental setup for photon condensation inside a microcavity plasma. A gas is placed inside a Fabry-Pérot cavity of distance d and transverse dimension $w \gg d$. The microplasma is created by an electrical discharge that ionizes the gas. A laser is shined perpendicular to the cavity mirrors, so that a total number of N_{ph} photons is stored inside. The inset shows a schematic representation of the longitudinal spectrum of a $d = 100 \mu\text{m}$ microcavity with plasma density $n_e = 10^{14} \text{cm}^{-3}$.

$\omega_\ell \equiv \omega_{\mathbf{k}_\ell}$. We suppose that the transverse dimension of the cavity w verifies $w \gg d$ so that transverse modes form a wave-vector continuum with a small contribution to the frequency. This results in recasting the Compton amplitude as

$$\int d^3\mathbf{k}' W(p, k \rightarrow p', k') \rightarrow \sum_{\ell'} \tilde{W}(p, k_\ell \rightarrow p', k_{\ell'}), \quad (12)$$

with \tilde{W} being the appropriate transition rate in terms of the discretized momentum.

Assuming thermal equilibrium for the plasma, the electron distribution is approximated by a Maxwell-Boltzmann function at temperature T_e , $F(\mathbf{k}) = F_0 \exp(-E_{\mathbf{k}}/k_B T_e)$, where $E_{\mathbf{k}} = \hbar^2 \mathbf{k} \cdot \mathbf{k} / (2m_e)$ is the electron dispersion and F_0 ensures the normalization $\int d^3\mathbf{k} F(\mathbf{k}) = n_e$. The electron equilibrium is assumed to be maintained throughout the experiment, such that $\partial_t F \simeq 0$ is valid during the photon equilibration process. The Boltzmann equation can then be simplified to the following balance equation

$$\partial_\tau N_\ell = \sum_{\ell'} [N_{\ell'} \mathcal{W}_{\ell\ell'} - N_\ell - (1 - \mathcal{W}_{\ell\ell'}) N_\ell N_{\ell'}], \quad (13)$$

with $N_\ell \equiv N(\mathbf{k}_\ell, \tau)$ the photon-mode occupancies [29]. Here, $\Delta_{\ell\ell'} = \hbar(\omega_{\ell'} - \omega_\ell) / (k_B T_e)$ are normalized energy shifts and $\mathcal{W}_{\ell\ell'} = \exp(\Delta_{\ell\ell'})$. Moreover, $\tau = t/\tau_c$ with $\tau_c = 8\pi / (\sigma_T n_e c)$ being the Compton time.

The last term on the right-hand side of Eq. (13) vanishes as $T_e \rightarrow \infty$, and the equation becomes linear in N_ℓ , which prevents the formation of a condensate [30,31]. Hence, there must be a critical temperature T_c above which the condensate no longer develops. In cold atom experiments, the value of T_c typically ranges between a few nK and μK , depending on the density and mass of the atomic cloud [32]. In fact, theoretical calculations reveal that T_c scales as $T_c \sim 1/m$, with m typically in the range 10^{-27} – 10^{-26} kg for atomic BECs. In the present case, the photon mass is about 12–14 orders

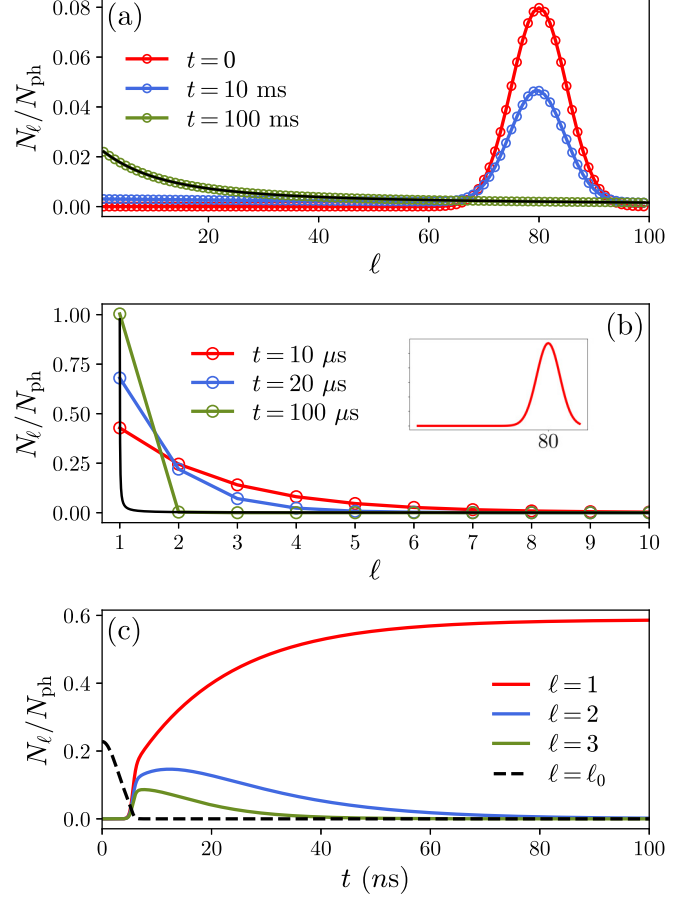


FIG. 2. Photon spectra for the two distinct phases with $N_{\text{ph}} = 10^8$: (a) $T_e = 10^5 \text{eV}$ ($T_e > T_c$) with steady-state Bose-Einstein distribution; (b) $T_e = 3 \text{eV}$ ($T_e < T_c$) with the formation of a condensate. The inset shows the initial distribution and the solid black lines show the Bose-Einstein distribution at the plasma temperature, after the system had reached thermal equilibrium. (c) Time evolution of the mode occupancies displaying condensation, with $N_{\text{ph}} = 10^{11}$ and $T = 3 \text{eV}$. Other parameters are $d = 100 \mu\text{m}$, $n_e = 10^{14} \text{cm}^{-3}$, $\ell_0 = 80$, and $\Gamma = 5$.

of magnitude below the typical atomic masses. We can thus anticipate much higher critical temperatures.

Thermalization and condensation. Solutions to Eq. (13) have been obtained numerically, using a fourth-order Runge-Kutta method. The occupancies were initiated with a Lorentzian distribution centered at $\ell = \ell_0$, with bandwidth Γ and total number of photons N_{ph} ,

$$N_\ell(0) = \frac{N_{\text{ph}}}{\pi} \frac{\Gamma/2}{(\ell - \ell_0)^2 + (\Gamma/2)^2}. \quad (14)$$

Figure 2 shows the initial, intermediate, and steady-state occupancies as a function of the mode number, for the case of thermal and condensate steady states. In the steady state, the photon spectrum tends to a Bose-Einstein distribution,

$$f(\varepsilon, T, \mu) = \frac{1}{\exp\left(\frac{\varepsilon - \mu}{k_B T}\right) - 1}, \quad (15)$$

with $T = T_e$, signaling that photons have thermalized with the plasma.

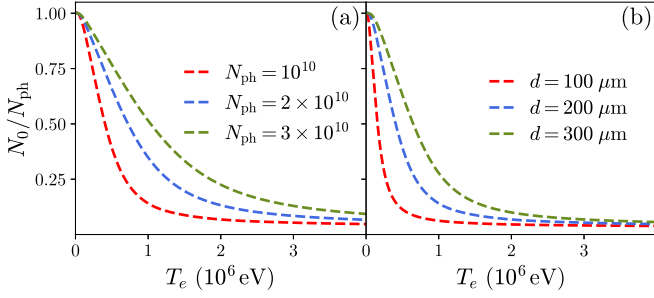


FIG. 3. Condensate fraction as a function of the electron temperature for a $n_e = 10^{14} \text{ cm}^{-3}$ microplasma: (a) fixed cavity length $d = 100 \mu\text{m}$, (b) fixed number of photons $N_{\text{ph}} = 10^{10}$.

The condensation time depends nonlinearly on N_{ph} , owing to the nonlinearity of the evolution equation (13). When the number of photons is small and the quadratic term can be discarded, the steady state is reached after a time of the order of $\tau_c \sim 1 \text{ s}$. When N_{ph} increases, the nonlinear term starts to dominate and the condensation time becomes a function of N_{ph} that is always smaller than τ_c . In Fig. 2(c) we show the time evolution of several mode occupancies with $N_{\text{ph}} = 10^{11}$, for which case the condensation time reaches tens of nanoseconds. The crossover between the BEC and thermal phases is governed by the chemical potential, which is fixed by the temperature and total numbers of particles through $N_{\text{ph}} = \sum_{\ell} f(\hbar\omega_{\ell}, T, \mu)$. The latter bears a solution of the form $\mu \equiv \mu(N_{\text{ph}}, T)$. When the number of photons surpasses a critical number N_c , the excess particles occupy the ground state, which is possible only if $\mu(N_{\text{ph}} > N_c, T) \sim \varepsilon_0$, with ε_0 the ground-state energy, so that Eq. (15) attains large values at the origin. In Fig. 3, we depict the condensate fraction as a function of T_e . The chemical potential was also determined numerically and the result is shown in the left panel of Fig. 4. It is also convenient to obtain an analytical estimate for T_c . The exact definition requires separating the contribution of the particles in the ground state from those in excited states, $N_{\text{ph}} - N_0 = \sum_{\ell \neq \pm 1} f(\hbar\omega_{\ell}, T, \mu)$. At the critical temperature,

we replace μ by ε_0 and neglect N_0 , to get

$$N_{\text{ph}} = g \sum_{\ell=2}^{\infty} f(\hbar\omega_{\ell}, T_c, \varepsilon_0), \quad (16)$$

where $g = 2$ is the degeneracy factor. Typically, an analytical estimate for T_c is available in the thermodynamic limit (in this case, that is $d \rightarrow \infty$ and $N_{\text{ph}} \rightarrow \infty$ while N_{ph}/d is maintained finite). However, as it has been recognized, the thermodynamic limit yields $T_c = 0$ when the spacial dimension of the condensate is less than three [33]. Although this prevents condensation from developing in very large systems, the result is modified when the system is considered finite. Therefore, instead of taking the thermodynamic limit, we simply assume that $d \gg c/\omega_p$ while being finite. As long as the energy spacing is negligible compared to the temperature, the summation in Eq. (16) can be replaced by an integral, and we obtain

$$T_c \approx \frac{\hbar^2 k_0^2}{\xi m_{\text{ph}} k_B} N_{\text{ph}}, \quad (17)$$

with $k_0 = \pi/d$ the ground-state wave vector and $\xi = 2\pi - 4 \arctan 2 \simeq 1.9$ a constant. The rigorous relation is obtained by evaluating Eq. (16) numerically, which we show in Fig. 4(b) for microcavity lengths.

As anticipated above, the value of T_c is much higher than that of atomic BECs, stemming from the small photon mass. For large d , the photon dispersion approaches $\varepsilon_k \simeq m_{\text{ph}} c^2 + \hbar^2 k^2 / (2m_{\text{ph}})$, which is quadratic, akin to Schrödinger bosons [34]. Additionally, Eq. (17) gives $T_c = 0$ when $d \rightarrow \infty$ and N_{ph}/d is finite, due to the dependence on N_{ph}/d^2 . This is consistent with previous investigations on finite-sized BECs [35].

Conclusions. We derived a kinetic model for the evolution of one-dimensional photon modes in contact with a plasma, starting from the Boltzmann equation. The electron population is considered to be in constant equilibrium at temperature T_e , which modifies the photon dispersion (by opening a gap of $\hbar\omega_p$ at $k = 0$) and thermalizes the photon gas due to multiple Compton scattering. Our results showed that the photon gas approaches a Bose-Einstein distribution at the plasma temperature, which admits a finite-sized condensed phase for sufficiently small temperatures. These temperatures are, however, much higher than the typical values for customary BEC. More importantly, we showed that these critical temperatures can be made larger than typical microplasma temperatures. The reason lies on the much smaller photon masses for the present configuration, $m_{\text{ph}} \simeq 10^{-40} \text{ kg}$. The condensation time decreases nonlinearly with increasing photon numbers, and can also be made small enough to overcome resonant absorption and cavity losses.

Experimental implementation of photon condensation as described here requires resonators with a high-quality factor Q . By estimating the photon lifetime inside the cavity we obtain restrictions on the quality factor that are compatible with the existing state-of-the-art technology ($Q \sim 10^4$, check the Supplemental Material for details [36]). The timescales of photon losses due to bremsstrahlung absorption and angular deflection can also be made much larger than the condensation time. In particular, the absorption coefficient can be reduced

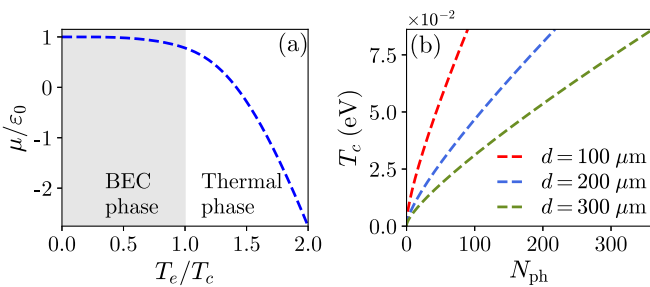


FIG. 4. (a) Typical chemical potential normalized profile as a function of the electron temperature. The BEC phase is the region of almost constant μ ; when μ decreases, the system enters in the thermal phase, with distribution spectrum of a thermal Bose gas. (b) Critical temperature as a function of the total number of photons for different cavities and $n_e = 10^{14} \text{ cm}^{-3}$. The critical temperature approaches a straight line for $d \gg c/\omega_p$.

to less than 1%. Moreover, electric discharge in a gas can be used to obtain a homogenous plasma of about 100–500 μm size as required for the thermalization [37]. To prevent mirror damage, the plasma should be contained inside a transparent cell. The latter may induce quantitative corrections to the quality factor, which can be compensated by the intensity of the laser [36].

The present work differs from the conventional case of photon condensation in dye-filled microcavities [7–9], where the photon mass is determined by the cavity cutoff frequency, typically in the range of 10^{14} Hz. Here, the plasma frequency establishes even smaller photon masses, resulting in higher critical temperatures. On the one hand, the ground-state energy is determined by the cavity distance and plasma density, which gives an extra degree of control over the BEC

parameters and may have technological applications on the search for new light sources. On the other hand, the microplasma technology can be adapted to fit inside small circuits, which may allow direct implementation of the condensate in a future generation of photon-based devices. In particular, the condensate constitutes a potential candidate for a quantum battery [38,39]. Extensions to the case of solid-state degenerate plasmas, eventually leading to condensation of photons in a partially filled cavity, as well as the inclusion of the reservoir dynamics, deserve further investigation.

Acknowledgments. J.L.F. and H.T. acknowledge Fundação da Ciência e a Tecnologia (FCT-Portugal) through Grants No. PD/BD/135211/2017 and No. UI/BD/151557/2021, and through Contract No. CEECIND/00401/2018 and Project No. PTDC/FIS-OUT/3882/2020, respectively.

-
- [1] C. C. Bradley, C. A. Sackett, J. J. Tollett, and R. G. Hulet, *Phys. Rev. Lett.* **75**, 1687 (1995).
- [2] D. G. Fried, T. C. Killian, L. Willmann, D. Landhuis, S. C. Moss, D. Kleppner, and T. J. Greytak, *Phys. Rev. Lett.* **81**, 3811 (1998).
- [3] F. Pereira Dos Santos, J. Léonard, J. Wang, C. J. Barrelet, F. Perales, E. Rasel, C. S. Unnikrishnan, M. Leduc, and C. Cohen-Tannoudji, *Phys. Rev. Lett.* **86**, 3459 (2001).
- [4] G. Modugno, G. Ferrari, G. Roati, R. J. Brecha, A. Simoni, and M. Inguscio, *Science* **294**, 1320 (2001).
- [5] R. Y. Chiao and J. Boyce, *Phys. Rev. A* **60**, 4114 (1999).
- [6] J. Klaers, F. Vewinger, and M. Weitz, *Nat. Phys.* **6**, 512 (2010).
- [7] J. Klaers, J. Schmitt, F. Vewinger, and M. Weitz, *Nature (London)* **468**, 545 (2010).
- [8] S. Barland, P. Azam, G. L. Lippi, R. A. Nyman, and R. Kaiser, *Opt. Express* **29**, 8368 (2021).
- [9] J. Marelic and R. A. Nyman, *Phys. Rev. A* **91**, 033813 (2015).
- [10] J. Klaers, J. Schmitt, T. Damm, F. Vewinger, and M. Weitz, *Phys. Rev. Lett.* **108**, 160403 (2012).
- [11] D. N. Sob'yanin, *Phys. Rev. E* **85**, 061120 (2012).
- [12] D. W. Snoke and S. M. Girvin, *J. Low Temp. Phys.* **171**, 1 (2013).
- [13] P. Kirton and J. Keeling, *Phys. Rev. Lett.* **111**, 100404 (2013).
- [14] A. Kruchkov, *Phys. Rev. A* **89**, 033862 (2014).
- [15] A. Kruchkov and Y. Slyusarenko, *Phys. Rev. A* **88**, 013615 (2013).
- [16] C.-H. Wang, M. J. Gullans, J. V. Porto, W. D. Phillips, and J. M. Taylor, *Phys. Rev. A* **99**, 031801(R) (2019).
- [17] P. W. Anderson, *Phys. Rev.* **130**, 439 (1963).
- [18] P. W. Higgs, *Phys. Rev. Lett.* **13**, 508 (1964).
- [19] F. Englert and R. Brout, *Phys. Rev. Lett.* **13**, 321 (1964).
- [20] G. S. Guralnik, C. R. Hagen, and T. W. B. Kibble, *Phys. Rev. Lett.* **13**, 585 (1964).
- [21] J. T. Mendonça and H. Terças, *Phys. Rev. A* **95**, 063611 (2017).
- [22] Y. B. Zel'Dovich and E. V. Levich, *Sov. Phys. - JETP* **28**, 1287 (1969).
- [23] R. A. Sunyaev and Y. B. Zeldovich, *Astrophys. Space Sci.* **7**, 3 (1970).
- [24] J. G. Eden and S.-J. Park, *Plasma Phys. Controlled Fusion* **47**, B83 (2005).
- [25] J. Mendonca, *Theory of Photon Acceleration*, Series in Plasma Physics (CRC Press, Boca Raton, FL, 2000).
- [26] The cross section for scattering between charged particles and photons is proportional to Q^4/m^2 , where Q is the charge of the charged scatters and m its mass. Hence, the ratio between the probabilities for photon scattering with an ion and with an electron is of order Z^4s^2 , with Z the ionic charge in units of the elementary charge, and s the ratio between electron and ion masses. For a Ne plasma, the ratio of probabilities is of order 10^{-10} .
- [27] D. J. Eckstrom, H. H. Nakano, D. C. Lorents, T. Rothem, J. A. Betts, M. E. Lainhart, D. A. Dakin, and J. E. Maenchen, *J. Appl. Phys.* **64**, 1679 (1988).
- [28] M. Birkinshaw, *Phys. Rep.* **310**, 97 (1999).
- [29] Although Eq. (10) guarantees that the total number of photons is a conserved quantity, $\partial N_{\text{ph}}/\partial t = 0$, after invoking Eq. (12) this is no longer true. In reality, the approximation amounts to replacing the photon distribution by the distribution of longitudinal modes of lowest transverse mode, hence some variations are expected. In any case, we verified numerically that those variations never surpass 1% for the regions of interest.
- [30] C. D. Levermore, H. Liu, and R. L. Pego, *SIAM J. Math. Anal.* **48**, 2454 (2016).
- [31] C. Josserand, Y. Pomeau, and S. Rica, *J. Low Temp. Phys.* **145**, 231 (2006).
- [32] J. R. Anglin and W. Ketterle, *Nature (London)* **416**, 211 (2002).
- [33] R. Weill, A. Bekker, B. Levit, and B. Fischer, *Nat. Commun.* **10**, 747 (2019).
- [34] F. Dalfovo, S. Giorgini, L. P. Pitaevskii, and S. Stringari, *Rev. Mod. Phys.* **71**, 463 (1999).
- [35] W. Ketterle and N. J. van Druten, *Phys. Rev. A* **54**, 656 (1996).
- [36] See Supplemental Material at <http://link.aps.org/supplemental/10.1103/PhysRevE.108.L013201> for details on the microplasma production and experimental parameters, loss estimation and condensation time scales.
- [37] L. Lin, H. Quoc Pho, L. Zong, S. Li, N. Pourali, E. Rebrov, N. Nghiep Tran, K. K. Ostrikov, and V. Hessel, *Chem. Eng. J.* **417**, 129355 (2021).
- [38] F. C. Binder, S. Vinjanampathy, K. Modi, and J. Goold, *New J. Phys.* **17**, 075015 (2015).
- [39] D. Farina, G. M. Andolina, A. Mari, M. Polini, and V. Giovannetti, *Phys. Rev. B* **99**, 035421 (2019).